

UNIVERSITY GRANTS COMMISSION

FINAL REPORT SUBMISSION FOR MAJOR RESEARCH PROJECT

Title of the project

**INVESTIGATION OF FLOW MAL-DISTRIBUTION IN SILICON
BASED MICROCHANNEL HEAT SINKS**



Name of the Principal Investigator

**Dr. G. KUMARAGURUPARAN
ASSOCIATE PROFESSOR
DEPARTMENT OF MECHATRONICS
THIAGARAJAR COLLEGE OF ENGINEERING
MADRURAI- 625015
TAMILNADU.**

Title of the Research Project	: Investigation of Flow Mal-distribution in Silicon based Microchannel Heat sinks
UGC approval Letter No. and Date	: 43-444/2014(SR) and 28.09.2015

CHAPTER 1

INTRODUCTION

1.1 INTRODUCTION

Recent research initiatives have been focused to miniaturize the size and increase the efficiency of micro-chips and its leads to such a high heat generation level of 100 W/cm^2 that its temperature removal is major concern for safety and reliability of electronic devices. Heat must be removed in order to maintain the continuous operation. Conventional cooling such as heat sink with fin may not be sufficient to handle such high heat. Microchannel heat sink is a promising cooling technology to remove such a huge heat flux. Microchannel cooling technology was first put forward by Tuckerman and Pease (1981). Microchannel can be described as channel of dimensions less than 1 mm and greater than one micron. Microchannel provides advantage of high surface to volume ratio. Due to high surface area to volume ratio of microchannel heat transfer coefficient values rises to the measure of few thousand W/m^2 . Due to these properties, microchannel is widely used in electronic devices, micro heat exchangers etc.

1.2 MICROCHANNEL HEAT SINK COOLING

A number of cooling solutions have been developed to cool the microelectronic devices which include extended surface (fins), highly parallel air and liquid impingement systems, modular internal conduction enhancement, indirect and direct liquid cooling with water and dielectric coolants. It is seen in integrated circuits, as the size becomes smaller, removal of heat becomes more complicated since the same (or better) processing power is packed into a smaller package. It is necessary to remove this heat as effectively as possible, preferably using some cooling fluids. The efficient heat removal in the miniature scale (sub-mm) is difficult since convection is relatively weak. The discovery of microchannels as effective cooling solution and their implementation in a miniaturized heat sink is a potential enabler to continued miniaturization. A microchannel heat sink consists of micron sized channels and fins in a parallel arrangement are shown in Fig. 1.1.

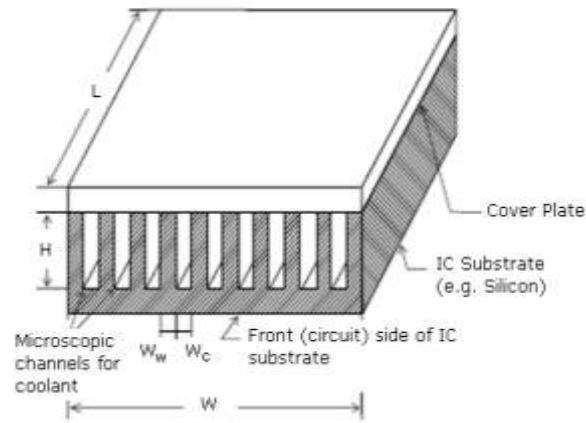


Fig. 1.1 High performance microchannel heat sink (without plenums)

For laminar, fully developed single phase flow at constant Nusselt number these small channel size (D_h) in microchannel heat sink gives high heat transfer coefficient

$$Nu = \frac{h D_h}{K} = \text{Constant} \implies h \propto \frac{1}{D_h}$$

Due to increased heat dissipation in microelectronic devices and miniaturization of microscale devices that require cooling, the flow passage dimensions in convective heat transfer applications have been shifting towards smaller dimensions. It is also seen that though smaller channel dimensions results in higher heat transfer performance, it is at the same time also accompanied by a higher pressure drop per unit length. Similarly non uniform flow distribution (flow maldistribution) through multiple channels is major issue in microchannel heat sinks.

This project deals with fabrication of silicon based microchannel heat sink and flow maldistribution studies in silicon based in microchannel heat sink.

CHAPTER 2

LITERATURE SURVEY

Tuckerman and Pease (1981) started the pioneer work of thermal management by experimentally demonstrating the high-performance heat sinking for very-large-scale integration (VLSI) systems. Bassiouny and Martin (1984) studied the flow distribution across the numbers of channels in U-type flow arrangement of Plate heat exchanger using axial velocity and pressure distribution in intake and exhaust conduits as the parameters for the generalized parameter (m^2) is taken as to describe the flow distribution. Todd M. Harms et al. (1999) studied experimentally about the microchannel having depth of the microchannel size $1000\mu\text{m}$. Single and Multiple channel microchannel cases were analyzed for Reynold's number range of 173 to 12900. The analysis shows that decreasing the channel width and increasing the channel depth provide better flow and heat transfer performance. Weilin Qu and Issam Mudawar (2002) investigated experimentally and numerically on Single phase microchannel heat sinks to find the pressure drop and heat transfer characteristics. They reported that the measured pressure drop and temperature distributions show good agreement with the corresponding numerical predictions.

Gian Luca Morini (2004) reviewed experimental results of single phase microchannel heat sinks. They mainly focused on the friction factor, laminar to turbulent transition and Nusselt number and reported that experimental data of the friction factor and of the Nusselt number in microchannels disagree with the conventional theory. Satish Kandlikar and William Grande (2003) reported surface tension becoming a dominant force in the flow field. Ming Chang Lu and Chi Chuan Wang (2006) studied the influence of inlet flow configurations in the microchannel heat sink. They studied numerically, the flow maldistribution and its heat transfer performance for five different flow configurations namely, I, Z, J, L, and T-arrangement. They reported, I-type has more mal-distribution at higher flow rates and it is decreased when increasing the number of channel. Z and L-type has the larger temperature difference, but no flow recirculation is attained for J-type arrangement. The J-arrangement showed good heat transfer performance at the lowest pressure drop is reported. Sean Ashman and Satish Kandlikar (2006) summarized the current fabrication process or techniques were used in microchannel fabrication for flow passages with hydraulic diameter of less than 200 micrometers. LIGA, Chemical Etching, Stereo lithography and micromachining were explained and compared these techniques related to tolerances material compatibility, and ease

of manufacturing. They reported that the most commonly used methods in the micro-machining category were diffusion bonding and diamond tool milling/grinding.

Satish Kandlikar and Clifford Hayner (2009) discussed the selection of the coolant type, cold plate type, channel configuration and their manufacturing issues. They reported that DI water is suggested and suitable corrosion inhibitor must be incorporated into the system. DI water without an inhibitor will attack any stress points (such as tube bends) and cause a leakage path with dire results.

John McHale and Suresh Garimella (2010) investigated the thermal entrance region of trapezoidal microchannel heat sinks for different aspect ratios. They have been chosen the silicon based microchannel side wall angles of 54.7° and 45° . The Local and average Nusselt numbers are reported as a function of dimensionless length and aspect ratio. They reported the new correlation for local and average Nusselt numbers.

Kumaraguruparan et al. (2011) studied experimental and numerical work on the disturbance in the uniform flow distribution in U-type microchannel heat sinks, considering the geometric parameters of channel width, depth, length and number of channel. They reported smaller channel width or depth or larger channel length can lead to more uniform flow distribution because of increase in the channel flow resistance. They noticed that the very small variations were occurred in the experimental results due to manufacturing tolerances of microchannel dimensions and impose significant random fluctuations in the channel-wise distribution of flow rates.

Manikanda Kumaran et al. (2013) studied the flow maldistribution with effect of the inlet and outlet location and the header shape design by numerically and experimentally. They reported, triangular inlet header provides better flow distribution; whereas, for the case of an outlet header, the trapezoidal header provides uniform flow distribution. They concluded that maldistribution decreases with header width.

Manoj Siva et al. (2014) experimentally investigated the influence of flow maldistribution on temperature distribution in parallel microchannel system that is supposed to have an adverse effect on hot spot formation in microelectronic devices. They varied the geometric parameter (channel hydraulic diameter), channel flow configurations (U,Z, I type) and chip power. They reported that flow distribution among the channels improved with a decreased in the channel hydraulic diameter due to higher pressure drop offered by each individual channels and also reported that higher pressure drop in $d = 88\mu\text{m}$ induces more uniform distribution compared to $d = 176\mu\text{m}$ resulting in a 3°C improvement in the standard

deviation of temperature on the chip surface and reduction in surface temperature. They concluded that chip surface temperature is higher for U type followed by Z and I type flow configuration because flow maldistribution is highest for U type and the least for I type.

Jose-Luis Gonzalez-Hernandez & Satish Kandlikar (2015) analyzed numerical work on microchannel cooling layer in 3D integrated circuited chips applications. A total of 21 configurations were simulated. The effect of varying the width and height of each of the microchannels on the overall performance was identified and discussed with total area of $10 \text{ mm} \times 10 \text{ mm}$, thickness of the walls is $100 \text{ }\mu\text{m}$ and total heat input 200W . They concluded that the higher height to width ratios lead to better overall performances.

Ravindra Kumar et al. (2015) reviewed the recent developments and methods to enhance the heat transfer performance of microchannels by using channel geometry, coolant and structural materials. They reported the Nano-fluid has the excellent potential to enhance the heat transfer performance in the field of single-phase liquid flow heat transfer. They reported the heat transfer coefficient and pressure drop are very much dependent on channel size, shape, arrangement of channels and fluid properties. For same geometric dimensions double layered microchannel heat sink provided about 6.3% higher thermal performance and lower pressure drop than the single-layer one is reported. They concluded that the thermal performance of the bifurcating microchannel heat sink is better than the corresponding continuous straight microchannel if the cooling system is designed properly.

Literature survey shows that, very less number of researchers focused in flow maldistribution and temperature maldistribution in microchannel heat sink.

2.1 Present Work:

This present work discuss about the fabrication of silicon based microchannel heat sinks and flow maldistribution study in the microchannel heat sinks by considering various hydraulic diameter, header size and header shape.

CHAPTER 3

OBJECTIVE AND METHODOLOGY

3.1 OBJECTIVE

The present investigation makes a detailed study on Microchannel heat sinks to attain the uniform flow distribution through multiple parallel microchannels. The major objectives of present work are listed in below,

- 1) To conduct flow maldistribution studies using software package, FLUENT
- 2) To optimize the shape of the flow header for obtaining uniform flow distribution.
- 3) To develop silicon based micro channel heat sink set up for conducting flow maldistribution analysis.

3.2 METHODOLOGY

The methodology adopted is outlined step by step,

- 1) Investigate flow maldistribution in microchannel heat sinks of different dimensions using the experimental facility, after performing flow simulation analysis using FLUENT
- 2) Optimize the dimensions of the channels and shape of flow header (which distributes coolant through multiple parallel channels) to reduce the flow maldistribution
- 3) Investigate the flow maldistribution in microchannel heat sink with optimized channel dimensions and flow headers of optimized shape
- 4) Fabricate silicon based microchannel heat sink using Deep Reactive Ion Etching (DRIE).
- 5) Develop an experimental facility with required measuring devices, pump, heater and sensor system.

CHAPTER 4

NUMERICAL ANALYSIS OF MICROCHANNEL HEAT SINKS

4.1 INTRODUCTION

In this chapter the numerical analysis of microchannel heat sink is discussed. The numerical analysis has been performed by using ANSYS Fluent 17.1 and modeling and meshes created using GAMBIT mesh generation software.

4.2 DESCRIPTION OF MODEL

Microchannel heat sinks (MCHS) with channels of rectangular cross section are analyzed. The schematic diagram of the microchannel heat sink is illustrated in Fig. 4.1. The size of the microchannel heat sink is $W=10\text{mm}$, $L=10\text{mm}$ and $H=0.3\text{mm}$. The corresponding inlet and outlet diameter is taken as 1mm. The numerical analysis is conducted for I Type inlet and outlet configurations) with constant hydraulic diameter $D_h=0.2\text{mm}$ (Hydraulic diameter $=\frac{2[\text{Channel width}*\text{channel depth}]}{(\text{Channel width}+ \text{channel depth})}$). Silicon is considered as the microchannel heat sink substrate. The wall thickness is 0.2mm. The thickness of the fin (s) is taken as 0.15mm. Numerical simulation was carried out for constant mass flow rate of 0.000105kg/s.

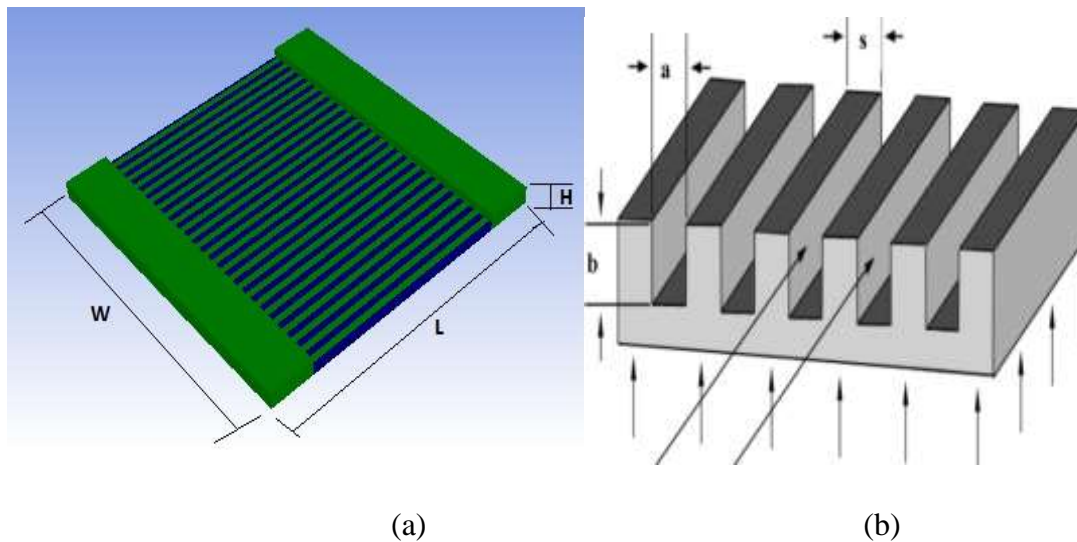


Fig. 4.1 (a) & (b) Schematic diagram of the Microchannel Heat Sink

In Fig. 4.2 (a), the inlet is at one side of the MCHS whereas the outlet is at the other side, and is termed as Z-shape arrangement. In Fig. 4.2 (b), both the inlet and outlet are at the opposite side is termed as I-type arrangement.

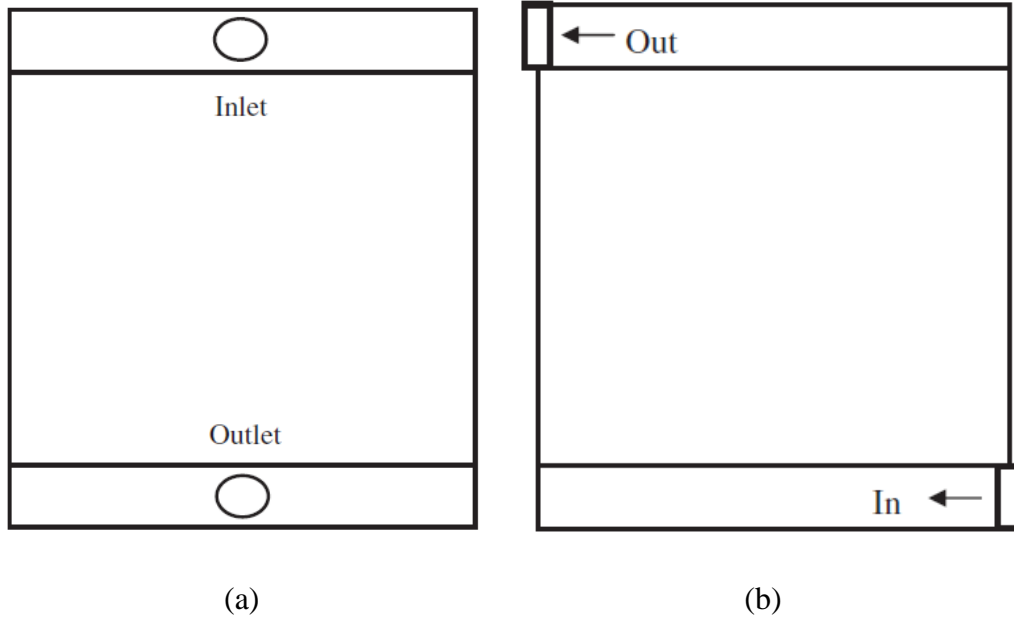


Fig. 4.2 (a) &(b)Schematic diagram of MCHS with I type Z type flow configuration

The following assumptions are made in the simulation of MCHS,

- Steady state flow
- Incompressible fluid
- Laminar flow
- Constant solid and fluid properties
- No slip condition

The governing equations for the fluid flow and microchannel heat sink include the mass conservation, momentum conservation, and the energy conservation equations.

Governing Equations:

Continuity Equation

$$\oint (V_j \cdot n_j) \cdot dA = 0$$

Momentum Equation

$$\rho \cdot V_{\text{cell}} \cdot \frac{\partial V_i}{\partial t} + \rho \oint (V_j \cdot n_j) \cdot dA = \rho \cdot g_i \cdot V_{\text{cell}} + \oint (\sigma_{ij} \cdot n_j) \cdot dA$$

Where the stress are given by

$$\sigma_{ij} = -p \delta_{ij} + \mu \left(\frac{\partial V_i}{\partial x_j} + \frac{\partial V_j}{\partial x_i} \right)$$

with δ_{ij} denoting the Kronekar delta and i, j denoting Cartesian directional indices.

4.3 NUMERICAL ANALYSIS OF FLOW MALDISTRIBUTION IN MICROCHANNEL HEAT SINKS

Fig. 4.2 shows the inlet & outlet flow configurations of Microchannel heat sink having inlet and outlet plenum dimensions of 13 mm × 1.5 mm × 0.3 mm, 33 number of microchannels with channel width 0.150 mm and depth 0.3 mm for I-type flow configuration for the mass flow rate of 0.000105 kg/s, flow distribution along the channels is relatively small. The micro rough surfaces present over the entire surface of channel walls were not included in the numerical analysis due to the difficulties in modeling of such features.

The flow maldistribution found to be existing in zig zag pattern which is maximum towards the middle of the microchannel heat sink nearer to the header inlet. The flow maldistribution is found to be minimal towards the micro channels at the right and left extremes which indicates the presence of flow mal distribution in the micro channel heat sink.

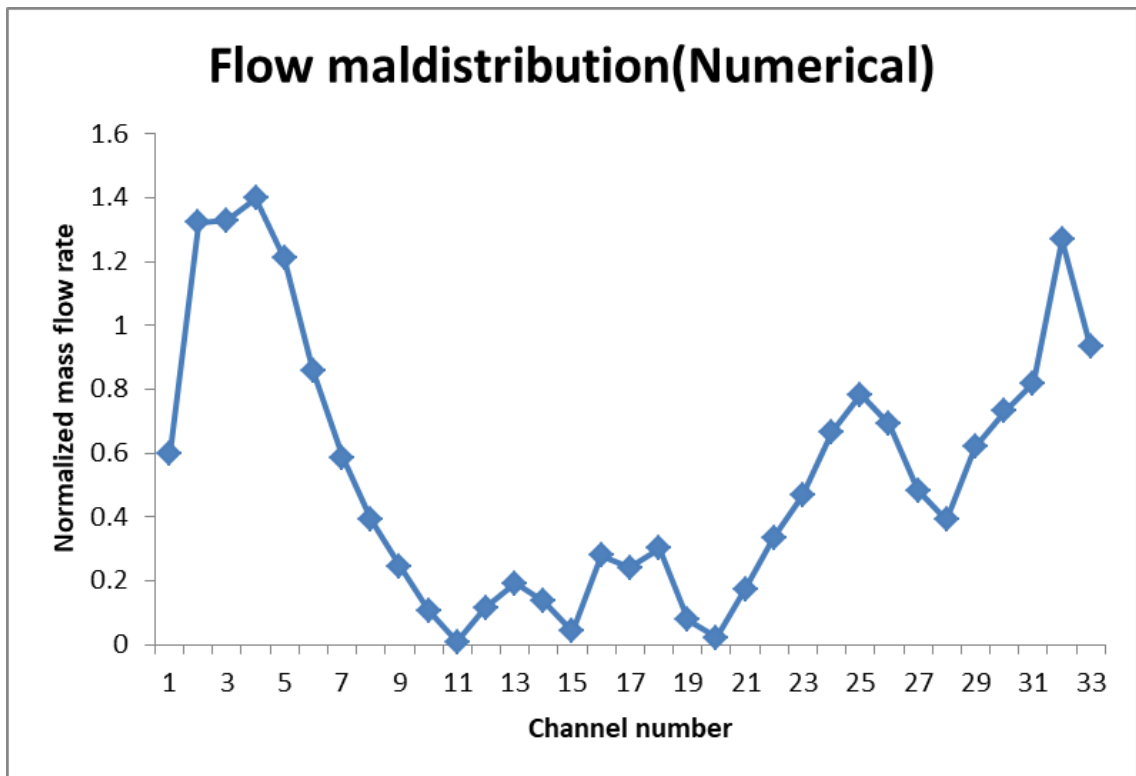


Fig. 4.3 Flow distribution for I-type flow

CHAPTER 5

FABRICATION OF MICROCHANNEL HEAT SINKS

5.1 INTRODUCTION

In this chapter fabrication of silicon based microchannel heat sinks is discussed. The fabrication of silicon based microchannel heat sinks has been done by Deep Reactive Ion Etching Process (DRIE) at CeNSE lab, Indian Institute of Science (IISc), Bangalore.

5.2 MICROCHANNEL FABRICATION PROCESS FLOW

Fig. 5.1 shows the fabrication process of silicon based microchannel heat sinks.

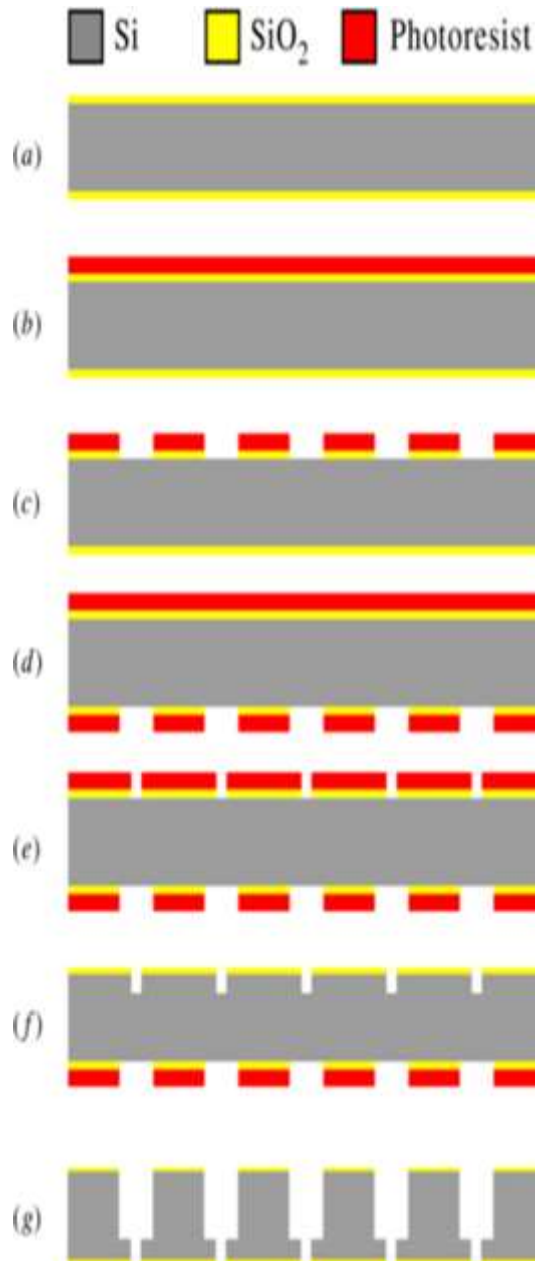


Fig. 5.1. MEMS fabrication process

The fabrication of silicon based microchannel heat sinks was carried out at the class 10 Micro Electro Mechanical Systems (MEMS) fabrication facility available at CeNSE lab, Indian

Institute of Science (IISc), Bangalore. The Process Flow for Micro channel heat sink fabrication is indicated in Fig. 5.2.

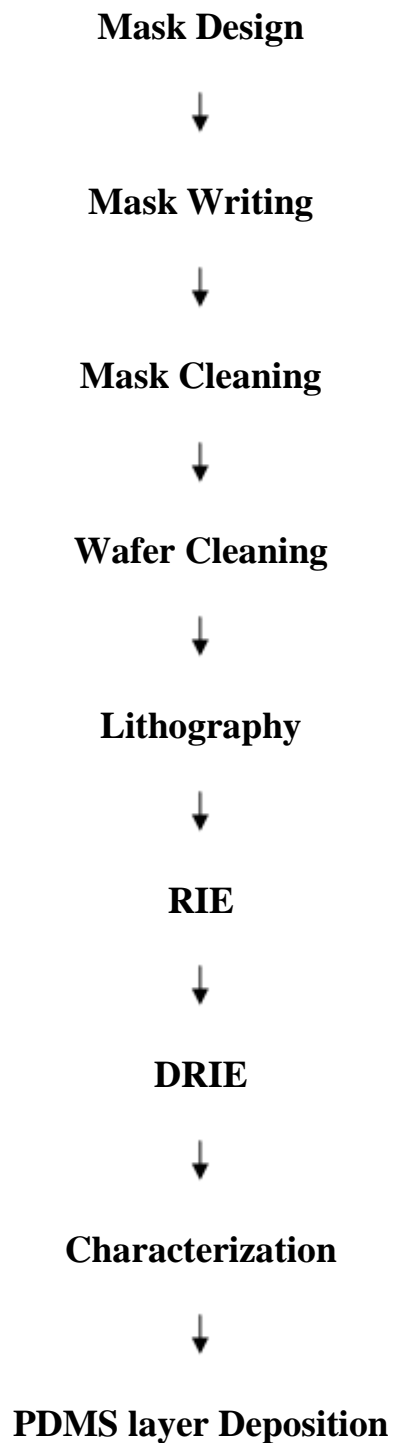


Fig 5.2 Process Flow of Micro channel heat sink fabrication

5.2.1 SILICON (SI) WAFER DETAILS

Two 4" pre oxidized silicon wafers each 500 μm thick were provided. The wafers were SSP polished and had a resistivity of 100 $\Omega / \text{sq.cm}$. The oxide layer deposited over the silicon wafers are measured using Ellipsometer. The oxide thickness was found to 1089 nm and 1092 nm for the first and second wafers respectively.

5.2.2 MASK DETAILS

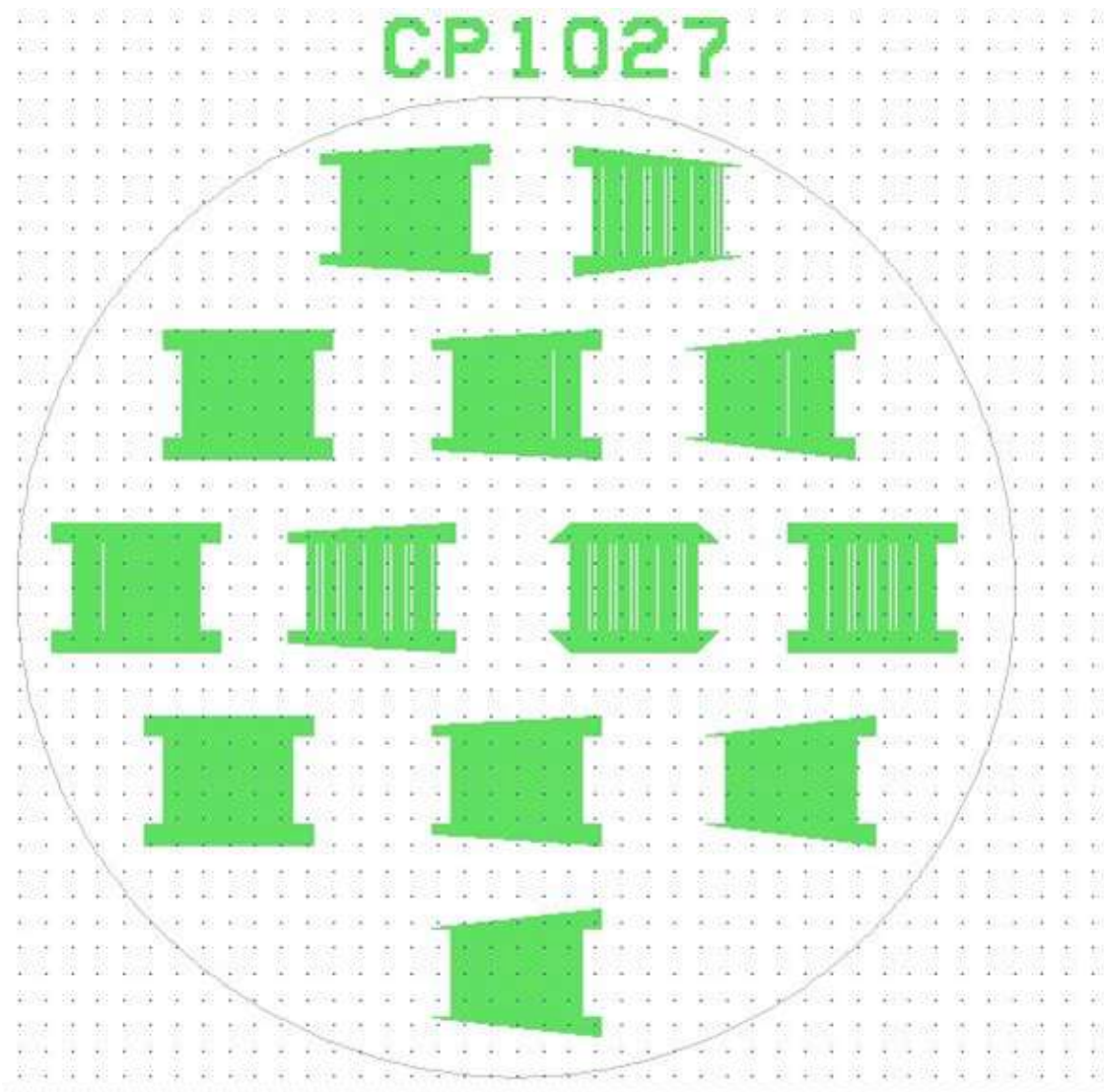


Fig. 5.3 Pattern to be etched made using CLEWIN

The mask design was done using Clewin Software. Total number of 13 designs with varied feature sizes and geometries were created and the patterns are mentioned in Fig. 5.3. Same mask design is used to etch both the wafers. The details of the mask design are listed in the Table 5.1.

Table 5.1 Dimensional and geometric features of mask designed

Sl.no	Channel width	Number of channels	Header shape	Header height	Channel height
1	200 μm	25	Rectangular	350 μm	350 μm
2		25	Trapezoidal		
3		25	Triangular		
4		25	Double Side Trapezoidal		
5	150 μm	33	Rectangular	350 μm	350 μm
6		33	Trapezoidal		
7		33	Triangular		
8	100 μm	50	Rectangular	350 μm	350 μm
9		50	Trapezoidal		
10		50	Triangular		
11	50 μm	99	Rectangular	350 μm	350 μm
12		99	Trapezoidal		
13		99	Triangular		

5.2.3 MASK WRITING

The mask was written on a silicate glass with 100nm thick chrome plating using laser aided mask writer. The mask was deposited with a 500nm thick layer of positive photo resist and the mask design done using the Clewin software was written to the mask using Mask writer Heidelberg.

5.1.4 WAFER CLEANING

The silicon wafers were cleaned to remove organic contaminants, using piranha cleaning in a solution of H_2O_2 and H_2SO_4 taken in a ratio of 1:3 for 10 minutes each. The Equipment used is level 2 bench. Then the wafers are dried using nitrogen for 3 minutes each. It is important for the wafer to be clean and free from contaminates since it will affect the successive process.

5.1.5 MASK CLEANING

The Mask was cleaned to remove Photo resist deposited over the mask, using acetone and IPA solutions for 8 minutes. Then the mask is piranha cleaned for 10 seconds. The

Equipment used is level 2 bench. Then the wafers are dried using dry nitrogen for 3 minutes each.

5.1.6 LITHOGRAPHY

The wafer was initially dehydrated for 10 to 20 minutes using a hot plate at 250°C and then allowed to cool for 2 to 3 minutes in ambient temperature.

A 1.4 μm thick AZ 5214E Photo resist is deposited over both silicon wafers by spin coating apparatus. After this the wafers are soft baked for 1 minute at 110°C to remove the solvent used in Photo resist completely.

Then the wafer is aligned with mask using EVG -620 mask aligner. Then a UV radiation of dosage 45mJ/m² is passed to the wafer through the mask, so that the exposed regions of the wafer get hardened. Developing of Photo resist is done using ME26A and the development time is 23 seconds.

Then the developed wafers are hard baked for one minute at a temperature of 110°C. After Lithography the developed patterns in the silicon wafers are checked for dimensions using a microscope and the picture of developed pattern is shown in Fig. 5.4. For an expected values of 50 microns 49.89 microns was obtained.

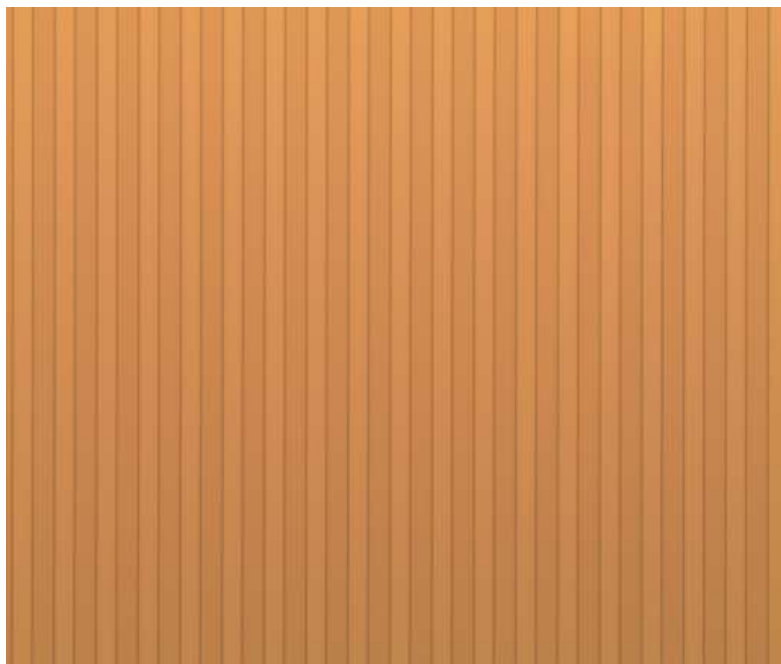


Fig. 5.4. 50 μm Channel view after Lithography on Photoresist

5.1.7 MASK OXIDE (SiO₂) ETCH

The Silicon dioxide (SiO₂) layer deposited over the Silicon wafer is to be etched using the photo resist pattern developed upon the SiO₂ layer through Reactive Ion Etching process. The photoresist pattern developed over the silicon di oxide layer during Lithography allows

etching the silicon di oxide mask layer in a selective way so as to develop the required pattern in original silicon wafer during Deep Reactive Ion Etching (DRIE) process.

The equipment used is RIE-F _Oxford (OI).First the chamber was cleaned with O₂ plasma followed by chamber conditioning and SiO₂ Etching. The Etchant gas used is CHF₃. The etch process is carried out at a rate of 200 nm/min for a duration of 6 minutes/wafer. After RIE Feature size of various configurations is measured using Leica Micro scope as shown in Fig. 5.5. The values of expected dimension after RIE is tabulated against the actual values obtained during RIE in Table.5.2



Fig. 5.5. 150 μm Channel view after RIE

Table 5.2. Post RIE feature size Measurement (Channel Width)

S.no	Expected Dimensions	Observed Dimensions
1	50 μm	60 μm
2	100 μm	110 μm
3	150 μm	160 μm
4	200 μm	217 μm

Equipment used: Leica Microscope

5.1.8 PR REMOVAL PROCESS

After RIE etching for sacrificial SiO₂ mask layer is completed the Photo resist pattern present over the Silicon wafer is removed using PR ash process in which each wafer is treated with O₂ Plasma in the plasma chamber for 4 minutes. The dimensions obtained in the sacrificial mask layer was observed as in Fig. 5.6

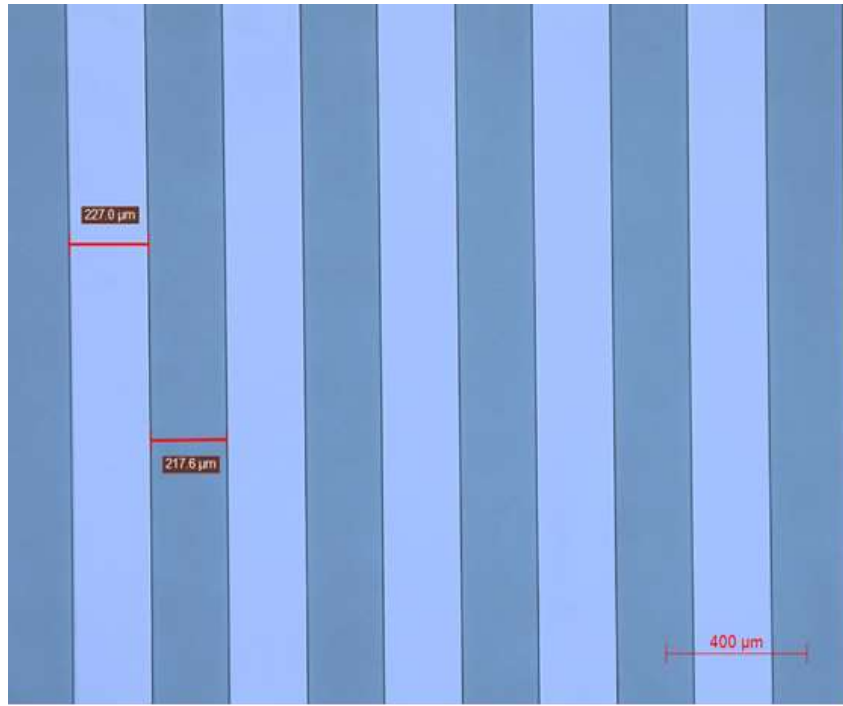


Fig. 5.6. 200 μm Channel view after PR ash

5.1.9 POST RIE STEP DEPTH MEASUREMENT

After oxide etching and Photo resist ash removal Post RIE Step Depth of the SiO_2 layer is measured using Dec Tak and it is shown in Fig. 5.7. The step depth is obtained as 1.108 μm & 1.152 μm for Sample -1 & Sample -2 respectively.

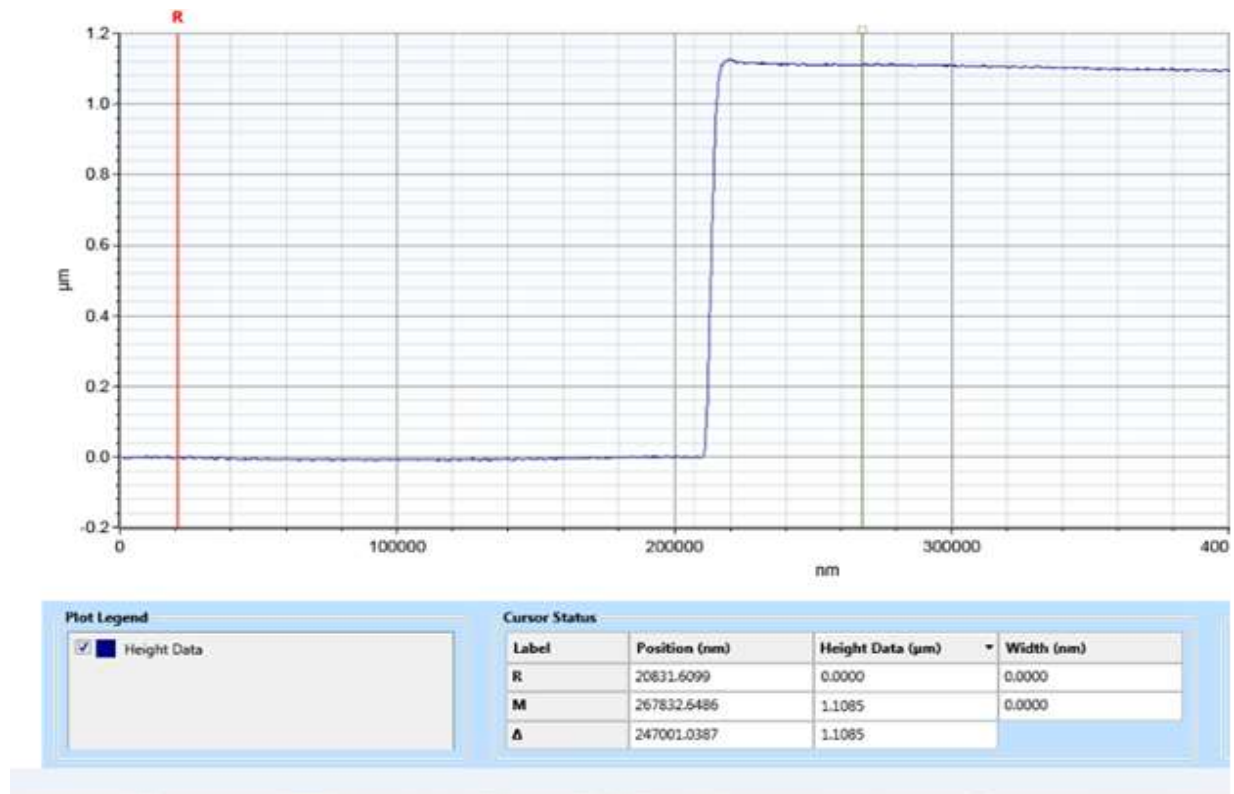


Fig. 5.7. Post RIE Step Depth measurement using Dec Tak

5.1.10 SILICON WAFER ETCH

The Silicon wafer with the etched pattern on it acts as the mask for etching silicon substrate below it. To etch the silicon Deep Reactive Ion Etching (DRIE) Bosch Dry Etch Process is used and it is done using DRIE_SPTS equipment. The total etch depth of 350 μm was etched at a rate of 33 $\mu\text{m}/\text{min}$. total time of 11min 30 sec was taken to complete etching for a single wafer. C_4F_8 gas was used for Deep Cycle and SF_6 gas was used for etch cycle.

5.1.11 SI ETCH INSPECTION

In order to check the obtained depth after DRIE, Step height measurement is used and the step heights of silicon etch is measured using Dek Tak microscope and it is shown in Fig. 5.8. For an Expected dimension of 350 μm . Dimensions obtained after DRIE of silicon wafer were 340 μm & 346 μm Sample 1 & Sample 2 respectively.

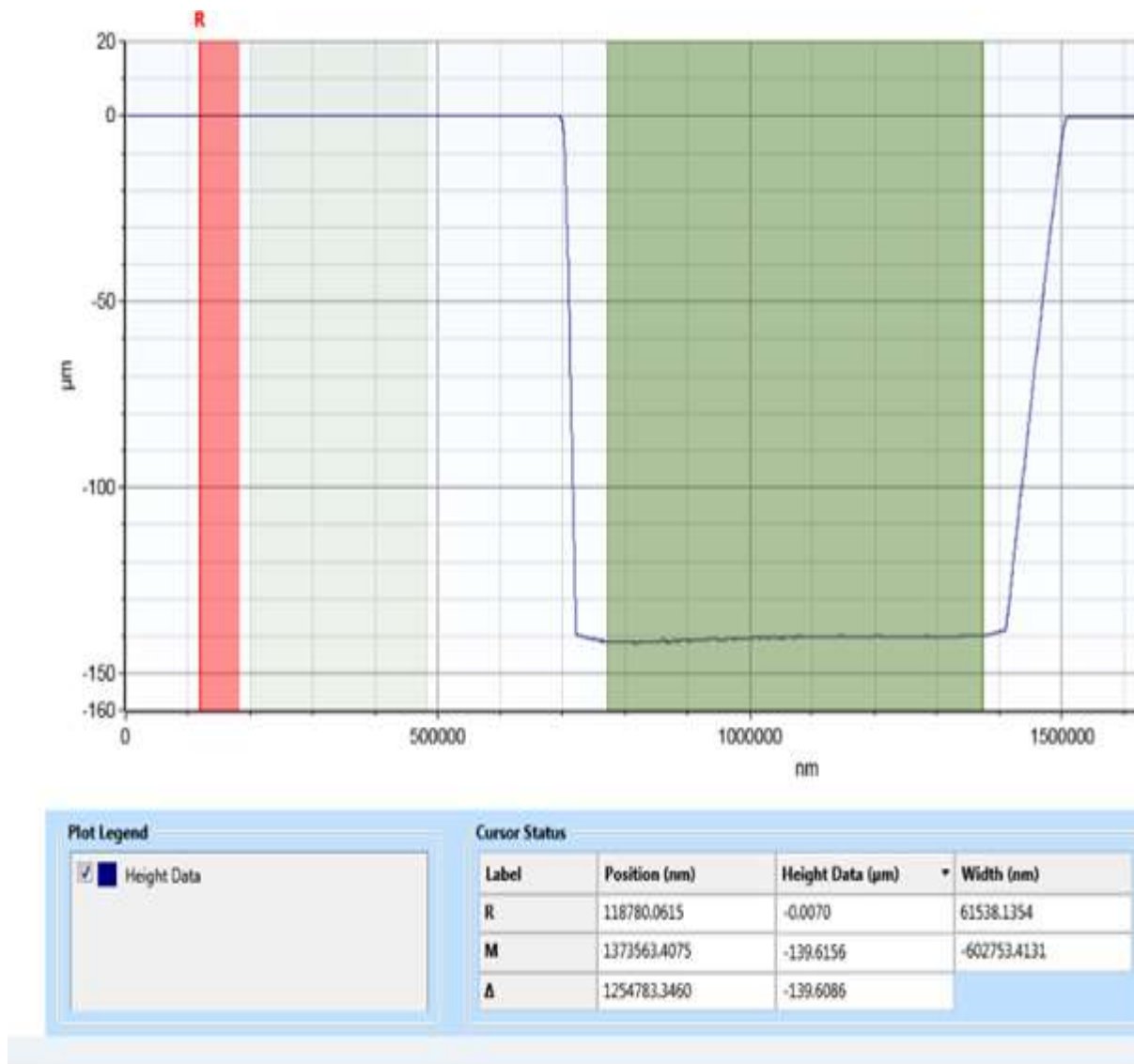


Fig. 5.8 Post DRIE Silicon step depth measurement using Dec Tak

5.1.12 POLY DIMETHYL SILOXANE (PDMS) BONDING

After completion of the channel etching now it's significant to seal the top of the Micro-channels and headers to make the fluid flow through the heatsink.

For this purpose PDMS bonding was tried in the Microfluidics lab at CeNSE, IISc and the picture of PDMS bonded Silicon microchannel heat sink is shown in Fig. 5.9. First the heat sink is was baked in the hot plate and then the PDMS sheet (premixed and hardened) was cut for required dimensions. Both PDMS and the heat sink are oxygen plasma treated in plasma chamber and then they are bonded with each other as soon as possible with a mild manual tapping to get the maximum bond strength.

Then the fluid flow was checked using Syringe pump available at Microfluidics laboratory IISc, Bangalore. The bonding between PDMS and Heat sink was found to be effective for very low flow rates. However for higher flow rates other effective solutions such as Pyrex sheet bonding, Anodic bonding, etc. are to be explored.



Fig. 5.9. PDMS layer bonded with Silicon substrate

CHAPTER 6

EXPERIMENTAL SETUP AND MEASUREMENT PROCEDURE

The experimental setup of the 33-channel heat sink with right-trapezoidal header employed for the study is shown in Fig. 6.1. The micro-channels and the headers are Surface micro machined over a silicon wafer of 0.5mm thickness using various techniques. The fabrication techniques employed for manufacturing the microchannel heat sink was discussed in detail. The surface of microchannels and header were sealed using an oxygen plasma treated PDMS layer in order to ensure the flow of fluid through the microchannel in the expected manner.

A transparent acrylic sheet along with manifolds to send working fluid through and to visualize the flow inside the channels and the header, was made using conventional machining techniques. Then the PDMS bonded heatsink was placed in a holding fixture and the manifold was set up over the heat sink in the required manner. The fluid was pumped using a low flow rate pump and the flow rate was measured using a flow meter. Water is used as the working fluid in the experiments. In order to quantify the mal-distribution encountered in the micro-channel setup, the flow taking place through each channels were captured by a high speed camera which can capture slow motion videos over a range of 30 to 500 fps with a considerable picture clarity. PDMS bonded Silicon microchannel heat sink with inlet and outlet manifold is shown in Fig. 6.2.

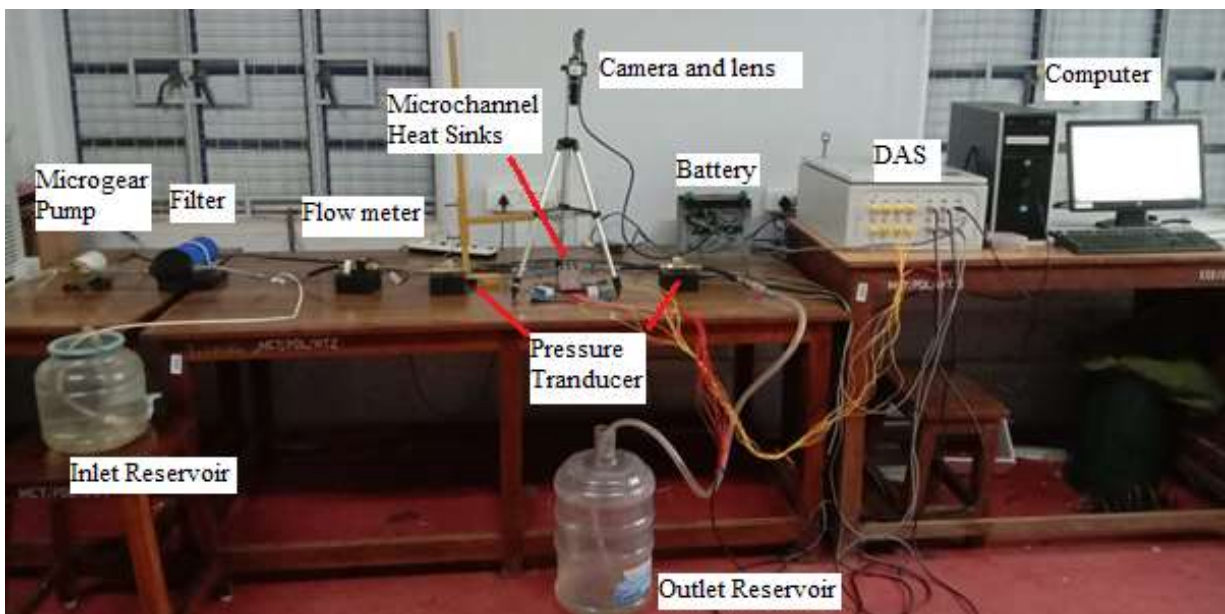


Fig. 6.1 Schematic layout of Experimental system

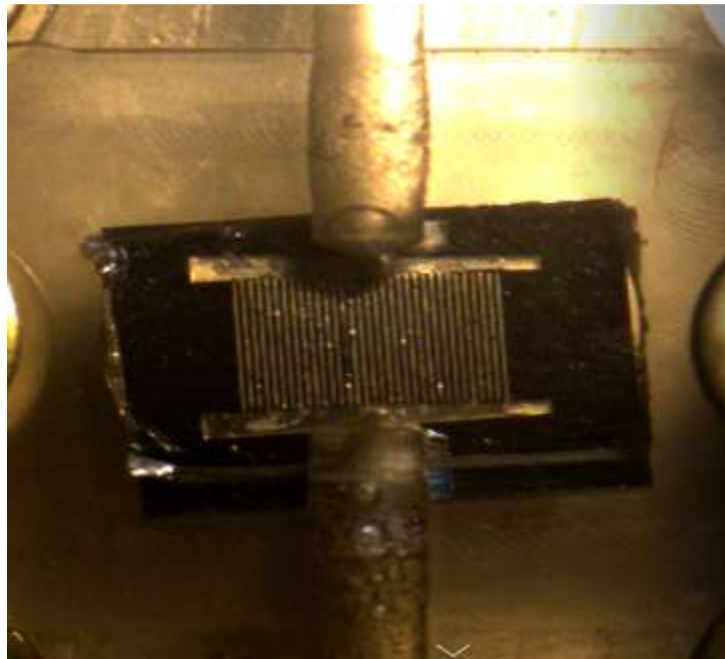
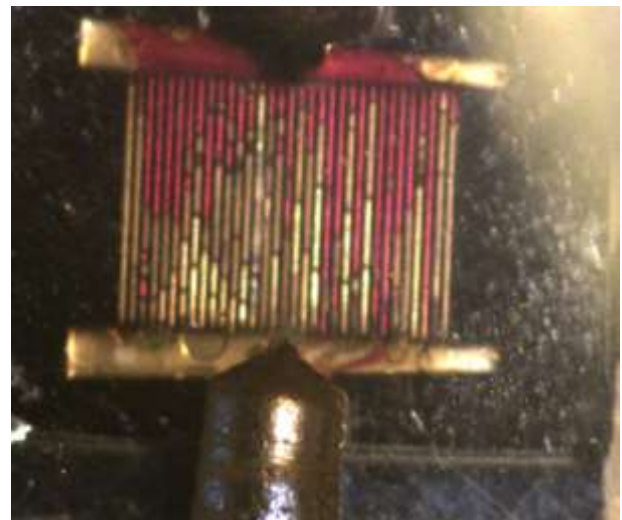


Fig 6.2 PDMS bonded Silicon microchannel with manifold



(a)



(b)

Fig 6.3 (a) & (b) Flow through individual channels at different time instants.

~ In order to create better color differentiation between the flow fluid and heat sink to study the flow maldistribution the working fluid was dyed with KMnO_4 . By extracting frames at different time instants the distance travelled by the fluid inside individual channels were measured and the picture of silicon based microchannel heat sinks with water+ KMnO_4 fluid is shown in Fig.6.3. It shows that, due to the nozzle and diffuser effect in the inlet header the flow of fluid is not passed uniformly in all channels.

CHAPTER 7

COMPARISON OF NUMERICAL AND EXPERIMENTAL RESULTS

The numerical analysis was performed as discussed in chapter 4 and the following outcomes were achieved. Using the flow data obtained normalized mass flow rate was calculated for each channel separately and was plotted against channel number in Fig. 7.1. The flow maldistribution found to be existing in zig zag pattern which is maximum towards the middle of the microchannel heat sink nearer to the header inlet. The flow maldistribution is found to be minimal towards the micro channels at the right and left extremes which indicates the presence of flow mal distribution in the micro channel heat sink.

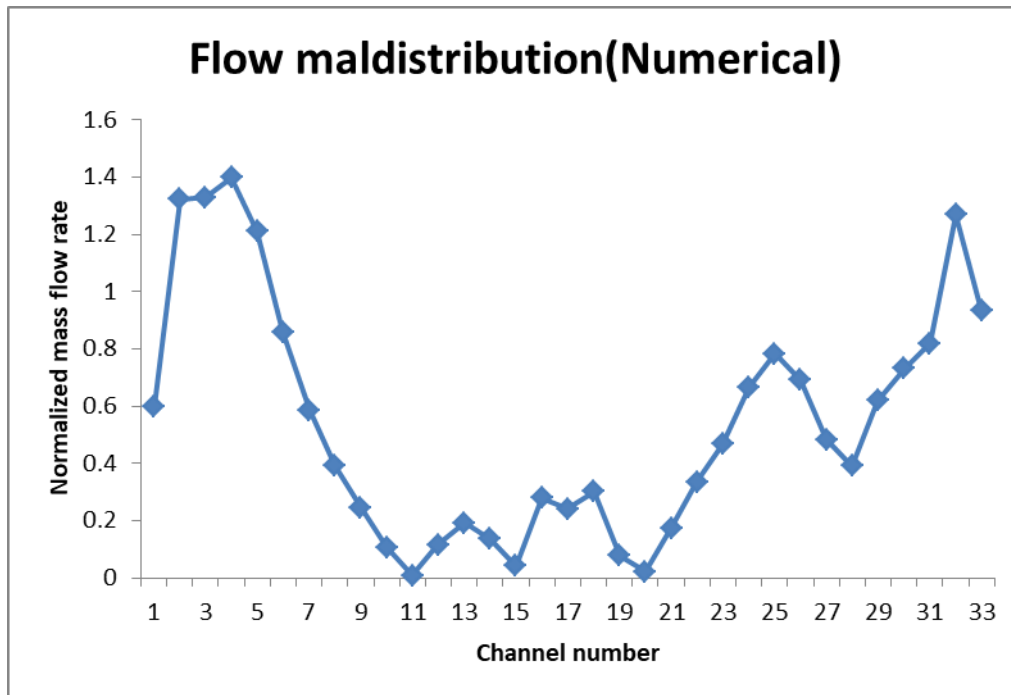


Fig. 7.1 Numerical analysis

. The results obtained in the experimental analysis is plotted in terms of normalized mass flow rate against the respective channel number in Fig 7.2. The result obtained indicates the zig zag nature of flow distribution among the channels. The flow profile looks much similar to that obtained in the numerical analysis but flow maldistribution was found to be existent over the channels in the center too. The flow pattern achieved during the experimental studies clearly indicate the presence flow maldistribution among the channels. These results were obtained for a very low mass flow rate of 6.3ml/min. The uniform mass flow rate is mentioned in Fig. 7.3 and also numerical and experimental results has been compared. It clearly states that, the flow maldistribution is occurred mainly in center of the microchannel heat sink due to nozzle and diffuser effect in the header.

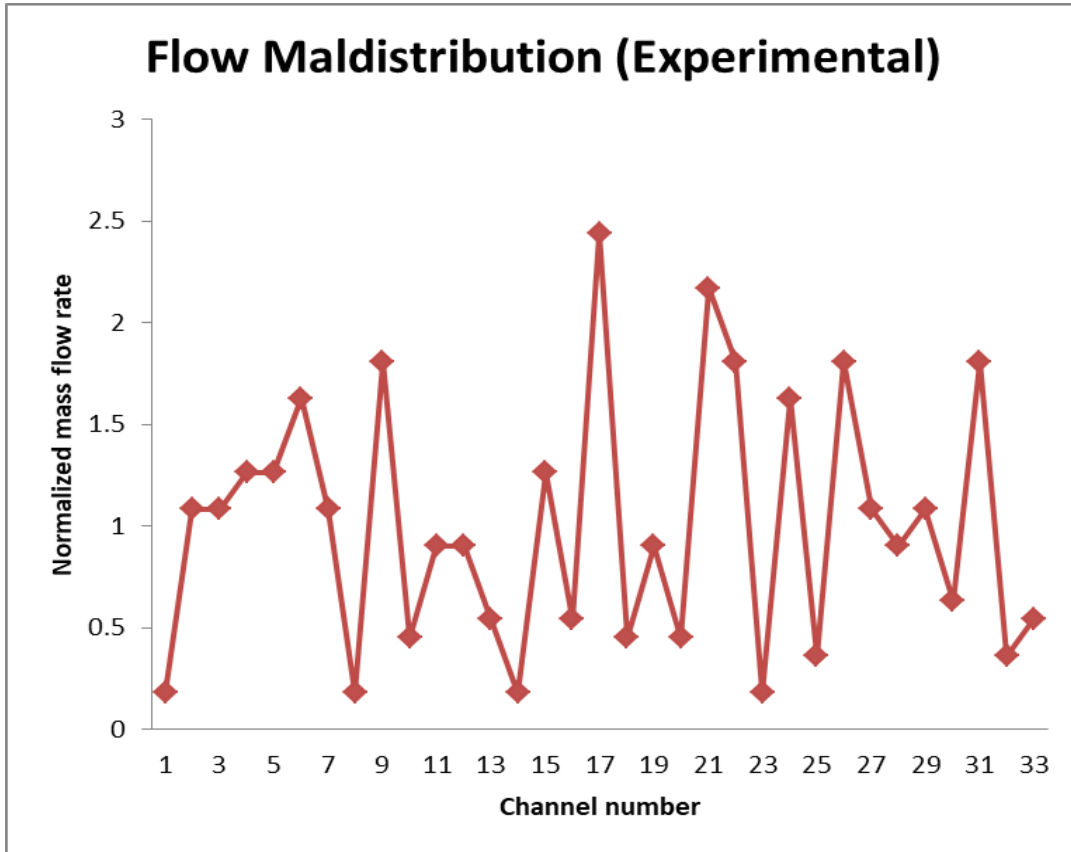


Fig. 7.2 Experimental analysis

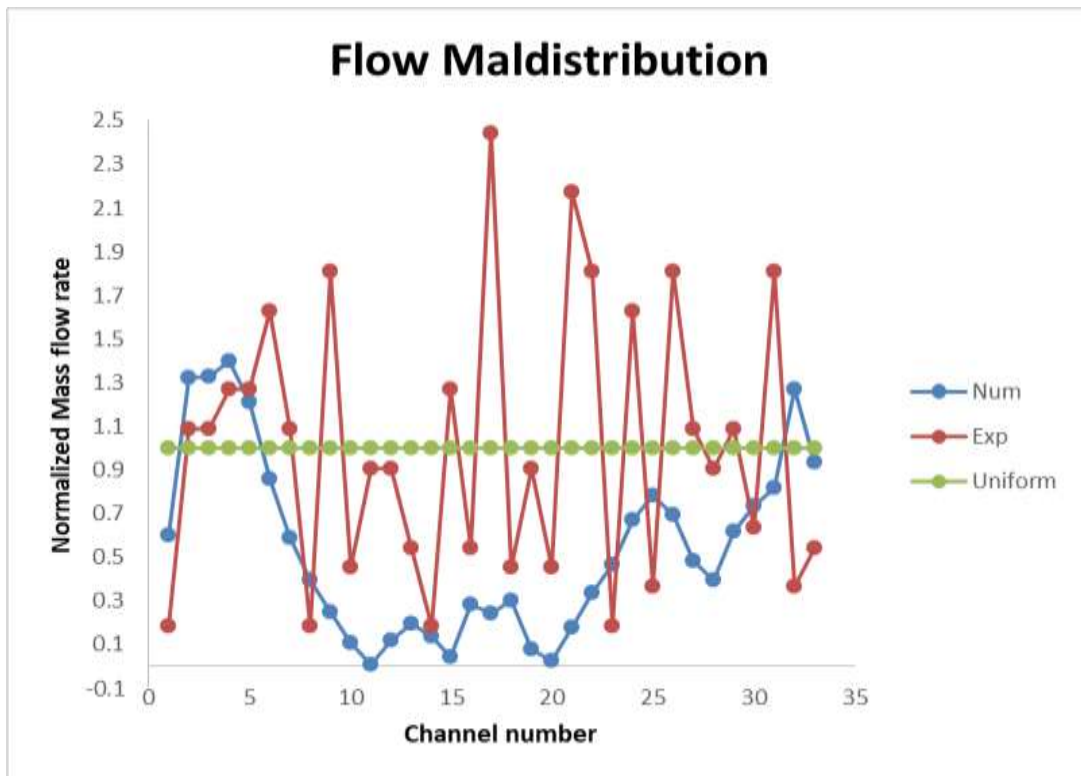


Fig.7.3 Comparison of Experimental data with numerical data

CHAPTER 8

CONCLUSION

The present study concentrates on the effects of header design on flow mal-distribution in a micro-channel (33 channels) heat sink. Experiments have been conducted to investigate the flow mal-distribution along the channel length and between the channels. The Flow mal-distribution was studied for I-type flow configuration in a microchannel heat sink with right trapezoidal header at inlet and outlet. Numerical simulations have been performed for Microchannel heat sinks (MCHS) with channels of rectangular cross section are analyzed. Size of the microchannel heat sink is $W=10\text{mm}$, $L=10\text{mm}$ and $H=0.3\text{mm}$. The corresponding inlet and outlet diameter is taken as 1mm . The numerical analysis is conducted for I Type inlet and outlet configurations) with constant hydraulic diameter $D_h=0.2\text{mm}$. Silicon is considered as the microchannel heat sink substrate. The wall thickness is 0.2mm . The thickness of the fin (s) is taken as 0.15mm . Numerical simulation was carried out for constant mass flow rate of 0.000105kg/s . Predicted results clearly illustrate that flow separation and recirculation bubbles occurring in the inlet header are primary responsible for the flow mal-distribution between the channels. To quantify the mal-distribution through the channels, the channel-wise flow rate predicted at the channel inlets and the Normalized mass flow rate was studied. Results highlight that flow distribution is existent in the microchannel in a Zig Zag pattern. Predicted results agree well with the measured experimental data.

REFERENCES

1. Tuckerman, DB & Pease, RFW 1981, "High-Performance Heat Sinking for VLSI", IEEE Electron Device Letters, Vol. 2, pp. 126-129
2. Bassiouny, MK & Martin, H 1984, "Flow Distribution and Pressure Drop in Plate Heat Exchangers-I", Chemical Engineering Science, Vol. 39, pp. 693-700.
3. Todd, M, Harms, Michael 1999, J, Kazmierczak & Frank, M, Gerner, "Developing convective heat transfer in deep rectangular microchannels", International Journal of Heat and Fluid Flow, Vol. 20, pp. 149-157.
4. Weilin Qu & Issam Mudawar 2002, "Experimental and numerical study of pressure drop and heat transfer in a single-phase micro-channel heat sink", International Journal of Heat and Mass Transfer, Vol. 45, pp. 2549–2565.
5. Gian Luca Morini 2004, "Single-phase convective heat transfer in microchannels: a review of experimental results", International Journal of Thermal Sciences, Vol. 43, pp. 631–651
6. Satish, G, Kandlikar & William, J, Grande 2003, "Evolution of Microchannel Flow Passages-Thermohydraulic Performance and Fabrication Technology", Heat Transfer Engineering, Vol. 24, pp. 3–17.
7. Ming-Chang Lu & Chi-Chuan Wang 2006, "Effect of the Inlet Location on the Performance of Parallel-Channel Cold-Plate", IEEE Transactions on Components and Packaging Technologies, Vol. 29, pp. 30-38.
8. Sean Ashman & Satish, G, Kandlikar 2006, "A Review of Manufacturing Processes for Microchannel Heat Exchanger Fabrication", Fourth International Conference on Nanochannels, Microchannels and Minichannels,
9. John, P, McHale & Suresh, V, Garimella 2010, "Heat transfer in trapezoidal microchannels of various aspect ratios", International Journal of Heat and Mass Transfer, Vol. 53, pp. 365–375.
10. Satish, G, Kandlikar & Clifford, N, Hayner 2009, "Liquid Cooled Cold Plates for Industrial High-Power Electronic Devices—Thermal Design and Manufacturing Considerations", Heat Transfer Engineering, Vol. 30, pp. 918–930
11. Kumaraguruparan, G, Manikanda Kumaran, R, Sornakumar, T & Sundararajan, T 2011, "A numerical and experimental investigation of flow maldistribution in a micro-channel heat sink", International Communications in Heat and Mass Transfer, Vol. 38, pp.1349–1353.
12. Manikanda Kumaran, R, Kumaraguruparan, G & Sornakumar, T 2013, "Experimental and numerical studies of header design and inlet/outlet configurations on flow mal-

distribution in parallel micro-channels”, Applied Thermal Engineering, Vol. 58, pp. 205-216.

13. Manoj Siva, V, Arvind Pattamatta & Sarit, K, Das 2013, “A Numerical Study of Flow and Temperature Maldistribution in a Parallel Microchannel System for Heat Removal in Microelectronic Devices”, Journal of Thermal Science and Engineering Applications, Vol. 5, pp. 1-9.
14. Jose-Luis Gonzalez-Hernandez & Satish, G, Kandlikar 2015, “Overall performance evaluation of embedded microchannel cooling layers for 3D architecture chips”, IEEE.
15. Ravindra Kumar, Mohd. Islam & Hasan, MM 2015, “Recent Trends, Challenges and Scope in Single-Phase Liquid Flow Heat Transfer in Microchannels - A Review”, Global Sci-Tech, Vol. 7, pp. 1-8.